Received 14 August 2017; revised 1 October 2017; accepted 5 October 2017. Date of publication 10 October 2017;
date of current version 20 December 2017. The review of this paper was arranged by Editor C. Bulucea.

*Digital Object Identifier 10.1109/JEDS.2017.2761451*

# Experimental Investigations of State-of-the-Art 650-V Class Power MOSFETs for Cryogenic Power Conversion at 77K

**YU CHEN, XIAO-YUAN CHEN (Member, IEEE), TAO LI, YING-JUN FENG, YANG LIU, QIN HUANG, MENG-YAO LI, AND LEI ZENG**

School of Engineering, Sichuan Normal University, Chengdu 610101, China

CORRESPONDING AUTHOR: X.-Y. CHEN (e-mail: chenxy44@sina.com)

This work was supported by the General Program for Applied Fundamental Research Project of Sichuan Province under Grant 2016JY0163.

**ABSTRACT** With consideration of both the operating properties from cryogenic MOSFETs and refrigerating costs from cryogenic refrigerators, this paper attempts to carry out the experimental tests and performance evaluations of state-of-the-art 650-V class MOSFETs, and thus to explore a possible design guideline for cryogenic power conversions at liquid nitrogen temperature. Three cryogenic operating behaviors of on-state resistances and breakdown voltages of five types of commercial power MOSFETs and on-state voltage across their built-in reverse diodes are tested from 300 K to 77 K. The measured on-state resistances obtained in low-current tests show almost double-exponential functional relations with the operating temperatures, while the other two cryogenic parameters are directly or inversely proportional to the operating temperatures. Moreover, cryogenic on-state resistance behaviors in high-current tests from 20 A to 90 A are also found to have double-exponential functional relations with the operating currents. Based on the experimental results and their fitted temperature-dependent and current-dependent functions, integrated evaluation of overall energy efficiency involved with refrigerating cost is presented to form a feasible design guideline for cryogenic power conversions. Finally, two 40-kW and 4-MW boost choppers are conceptually designed and discussed to verify the proposed design guideline for the use in various MOSFET-based cryogenic power conversions.

**INDEX TERMS** Cryogenic MOSFET, cryogenic power conversion, energy efficiency, liquid nitrogen.

## I. INTRODUCTION

Cryogenic operation of metal-oxide-semiconductor field effect transistors (MOSFETs) is generally highlighted for improved energy efficiency compared to their room-temperature counterparts [1]. This merit is derived mainly from the reduced drain-source on-state resistance at lower temperatures. Up to now, a number of theoretical and experimental studies have demonstrated the feasibility of cryogenic power MOSFETs for high-efficiency power conversions [2]–[11]. In particular, this so-called cryogenic power conversion is well suited to combine with high temperature superconducting (HTS) power devices having self-contained cryogenic environments [12]–[17]. For instance, a cryogenic DC-DC chopper was developed in [15] for energizing the HTS field winding in a 100-kW HTS generator at liquid nitrogen ($LN_2$) temperature (77 K); a cryogenic DC-DC chopper was designed in [17] for controlling the energy exchanges of on-board superconducting magnetic energy storage (SMES) device in a liquid hydrogen ($LH_2$) powered fuel cell vehicle. Cryogenic power MOSFETs in [15] and [17] were designed to be cooled by $LN_2$ at 77 K and gas hydrogen ($GH_2$) at 50-100 K, respectively. However, it should be noted that an undesired increment in the on-state resistance could be found if the MOSFETs are immersed directly in the $LH_2$ at 20 K, and an optimal temperature range might be at 50-100 K according to the experimental investigations in [18] and [19]. Therefore, the $LN_2$ could be a suitable refrigerating fluid for achieving a high efficiency in various MOSFET-based cryogenic power conversions [12]–[17], [20]–[22].

Moreover, thanks to unique advantages of extremely high current capacity and nearly zero internal resistance from advanced HTS inductors, replacing conventional copper inductor by HTS inductor could further improve the energy efficiency in a cryogenic power conversion system. For instance, by integrating HTS inductors, a 50-kW DC-AC inverter in [23] and a 40-kW DC-DC chopper in [24] were reported to have ultra-high efficiencies of about 99.5% and 99.9%, respectively. In this 40-kW chopper case, two cryogenic power MOSFETs are introduced to replace one power MOSFET and one power diode at room temperature (300 K). As a result, the total power dissipation of power electronic devices is reduced from about 163 W to 26 W. The resistive loss from conventional copper inductor is also reduced from about 104 W to 9 W when a HTS inductor is used.

Along with the reduced on-state resistance at lower temperatures, however, there exist two undesired performance degradations [18], [19], [25]. One is the decreased drain-source breakdown voltage of one cryogenic power MOSFET itself, and the other is the increased on-state voltage across its built-in reverse diode. The former one limits the maximum operating voltage for avoiding power electronic failures, while the later one aggravates the power dissipation if the diode is involved in circuit operations. Due to the higher on-state voltage and its resulting higher power dissipation inside the diode, it is favored to avoid the use of reverse diode attached to a commercial power MOSFET unit or simply replace a standalone power diode unit by cryogenic power MOSFET [17], [24].

To clarify the intrinsic mechanisms behind the phenomena of cryogenic power MOSFETs, a number of scientific works related to theoretical calculation, simulation modeling and prototype development have been reported in the last few decades [2]–[11], [26]–[28]. Some cryogenic characteristics have been initially clarified from the views of semiconductor materials and relevant theories. For instance, the reduced on-state resistance was found to be caused by the increased carrier mobility, while the reduced breakdown voltage came from the increased impact ionization efficiency at lower temperatures [5], [6], [9]. In the case of keeping the reduced on-state resistance, the reduced breakdown voltage could be improved to its room-temperature value by doubling the N-drift region length inside the MOSFET [29].

However, most of the currently existing theoretical and empirical formulas are in the field of power electronic devices [2]–[11], [26]–[29]. They are not easy to be implemented by those engineering technicians in the fields of power electronic software control and hardware design. Specifically, there is almost no universal rule or guideline for implementing a practical cryogenic power conversion design at present.

In addition to the lack of design rules for cryogenic power conversions, the merit of improved energy efficiency remains to be clarified when both the reduced power dissipation of cryogenic power MOSFETs and the increased refrigerating loss are considered [12]–[17], [23]. Even when the MOSFETs are integrated into the cryogenic environment from an existing HTS power device, the added operating cost of commercial refrigerators should also be considered to evaluate the overall energy efficiency.

Consequently, with consideration of both the cryogenic properties from commercial power MOSFETs and the refrigerating costs from cryogenic refrigerators, we attempt to carry out the experimental tests and performance evaluations of state-of-the-art 650 V class power MOSFETs and thus to explore a possible design guideline for cryogenic power conversions. The experimental testing principle and set-ups will be presented in Section II. The cryogenic operation of power MOSFETs from several semiconductor manufacturers will be updated in Section III for fitting several mathematical functions among the cryogenic operating parameters and environmental temperature. Based on the experimental results from a series of high-current tests at 20-90 A, application analyses and performance evaluations of cryogenic power MOSFETs will be carried out in Section IV by considering the refrigerating properties from commercial refrigerators. The design guidelines and considerations for MOSFET-based cryogenic power conversions will be discussed in Section V. The conclusions will be made in Section VI.

## II. EXPERIMENTAL TESTING PRINCIPLE AND SET-UPS

In the experiments, three cryogenic operating parameters are tested from 300 K to 77 K: 1) drain-source on-state resistance $R_{ds}$ and 2) drain-source breakdown voltage $U_{dsmax}$ inside a power MOSFET, and 3) on-state voltage $U_{diode}$ across its built-in reverse diode. The gate-source voltage $U_{gs}$ is set to 10 V for testing the $R_{ds}$, and set to 0 V for testing the $U_{diode}$ and $U_{dsmax}$, respectively. Figs. 1 and 2 show the schematic diagram and experimental set-ups.

To obtain a continuous temperature-changing environment from 300 K to 77 K, the back conductive plate of drain electrode inside the MOSFET is installed on the upper edge of a long copper cold-conduction strip (∼18 cm), while the lower edge of the strip is immersed in the $LN_2$ contained inside a cryogenic vessel. The whole assembly of the MOSFET and its equipped cold-conduction strip is then installed at the terminal of the moving shaft of a vertically-inverted stepper motor. During the tests, the MOSFET gets closer and closer to the liquid surface of the $LN_2$ along with the linear descending motion of the shaft, and finally immerses inside the $LN_2$.

To monitor the operating temperature of the MOSFET as accurately as possible, a standard four-probe method is used. A Pt100-type platinum resistance sensor is stuck to the surface of the back conductive plate of drain electrode, with each pin of the sensor welded with one current lead and one voltage lead. Subsequently, the two current leads and two voltage leads are connected with the constant-current output ports (1 mA) and varying-voltage input ports inside a thermometer.

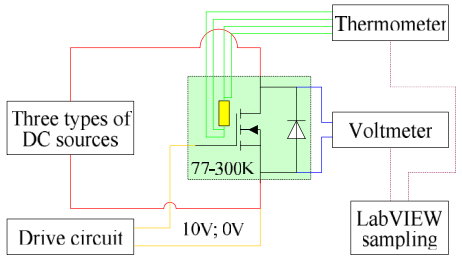


**FIGURE 1.** Experimental schematic diagram for testing the three cryogenic operating parameters inside a power MOSFET unit.

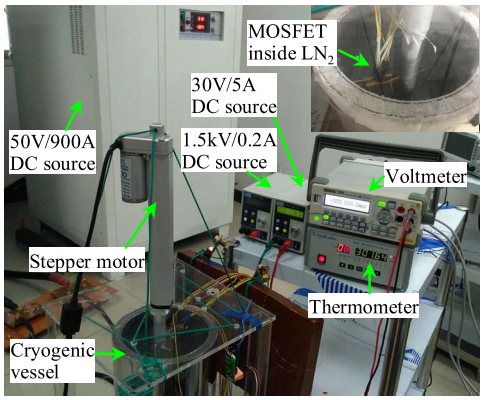


**FIGURE 2.** Photograph of the experimental testing set-ups.

As for the measurements of the three cryogenic operating parameters, three types of programmable DC sources are used. During the $R_{ds}$ and $U_{diode}$ tests, a 5-V/30-A DC source is controlled to output a constant current of 4 A to supply the MOSFET and its reverse diode operated from 300 K to 77 K. A voltmeter is then applied to measure the transient voltage across the drain electrode and source electrode of the MOSFET. Note that the $U_{diode}$ is equal to the measured voltage data directly, while the $R_{ds}$ can be indirectly obtained by dividing the constant current of 4 A. In addition to the above low-current tests, a series of high-current tests are also carried out for evaluating the long-time operating performance of the MOSFET at 77 K. The testing current from a 50-V/900-A DC source is ranged from 20 A to 90 A in the experiments.

During the $U_{dsmax}$ tests, initial output voltage and current of a 1500-V/0.2-A DC source are set as 750 V and 1 mA, respectively. When the breakdown voltage is reached (<750 V, at 77-300 K), the DC source is controlled automatically to output a constant current of 1 mA. Hence the measured voltage data from the voltmeter is the $U_{dsmax}$ that corresponds to the temperature changes. In the tests for the $R_{ds}$, $U_{diode}$ and $U_{dsmax}$, each power MOSFET is always powered on during the temperature changes from 300 K to 77 K. For simultaneous monitoring of the relations among the three cryogenic operating parameters and temperatures, a LabVIEW-based data acquisition system is used to collect the real-time data from the thermometer and voltmeter.

## III. CRYOGENIC BEHAVIORS AND THEIR FITTED MATHEMATICAL FUNCTIONS OF POWER MOSFETS

### A. CRYOGENIC BEHAVIORS OF POWER MOSFETS

In this work, five types of 650 V class power MOSFETs from various semiconductor manufacturers are used and numbered as follows: 1) Type A - X2-Class IXTX120N65X2 from IXYS; 2) Type B - Mdmesh$^{TM}$ STY145N65M5 from STMicroelectronics; 3) Type C - E-Series SIHS90N65E from Vishay; 4) Type D – SuperFET FCH023N65S3 from Fairchild / ON Semiconductor; 5) Type E - CoolMOS IPW65R019C7 from Infineon. Note that the above five MOSFETs have almost the highest continuous drain current capacities ($\geq$75 A) and lowest drain-source on-state resistances ($\sim$20 m$\Omega$) compared to other commercial counterparts with TO-247 or similar packages. Hence they suit to apply in various power conversions having relatively high current rating.

To further investigate the feasibility of cryogenic power conversions, the five MOSFETs are tested with regard to three cryogenic parameters of $R_{ds}$, $U_{dsmax}$ and $U_{diode}$. In the experiments, the five MOSFETs are firstly cooled down from 300 K to 77 K and then heated up from 77 K to 300 K. As shown in Fig. 3, their cryogenic behaviors obtained in the cooling down process and heating up process are basically overlapped. As for the small differences between the two processes, the reason might be that the measured temperature located near the surface of the MOSFET is suffered by different influences like ambient temperature, thermal conduction of the copper strip and moving speed of the stepper motor.

From Fig. 3, it can be seen that both the $U_{dsmax}$ and $U_{diode}$ have nearly linear correlations with the operating temperature $T$. Specifically, the $U_{dsmax}$ varies directly with temperature while the $U_{diode}$ varies inversely with temperature. These two undesired performance degradations should be practically considered in the design of cryogenic power conversions. As for the cryogenic on-state resistance behaviors, the five MOSFETs show almost linear descending trends when the operating temperature is not very low. These phenomena match well with the temperature-dependent on-state resistance curves given in the official data sheets. However, along with the further reduction in temperature, the descending rate of on-state resistance becomes slower and slower, and then the lowest on-state resistance will be reached at a certain temperature. As shown in the enlarged data curves in Fig. 3(a), (d), (g), (j) and (m), this optimal temperature value might be changed in different types of power MOSFETs due to their different temperature-dependent behaviors. Nevertheless, obvious reductions in the on-state resistance can be easily found in this experiment and other previous works such as in [2]–[11], [18], and [19]. These phenomena reveal the fact that cryogenic power MOSFETs are certainly with reduced power dissipation for themselves. However, we have to be aware that some certain increments in the on-state resistance appear when the operating temperature is lower than

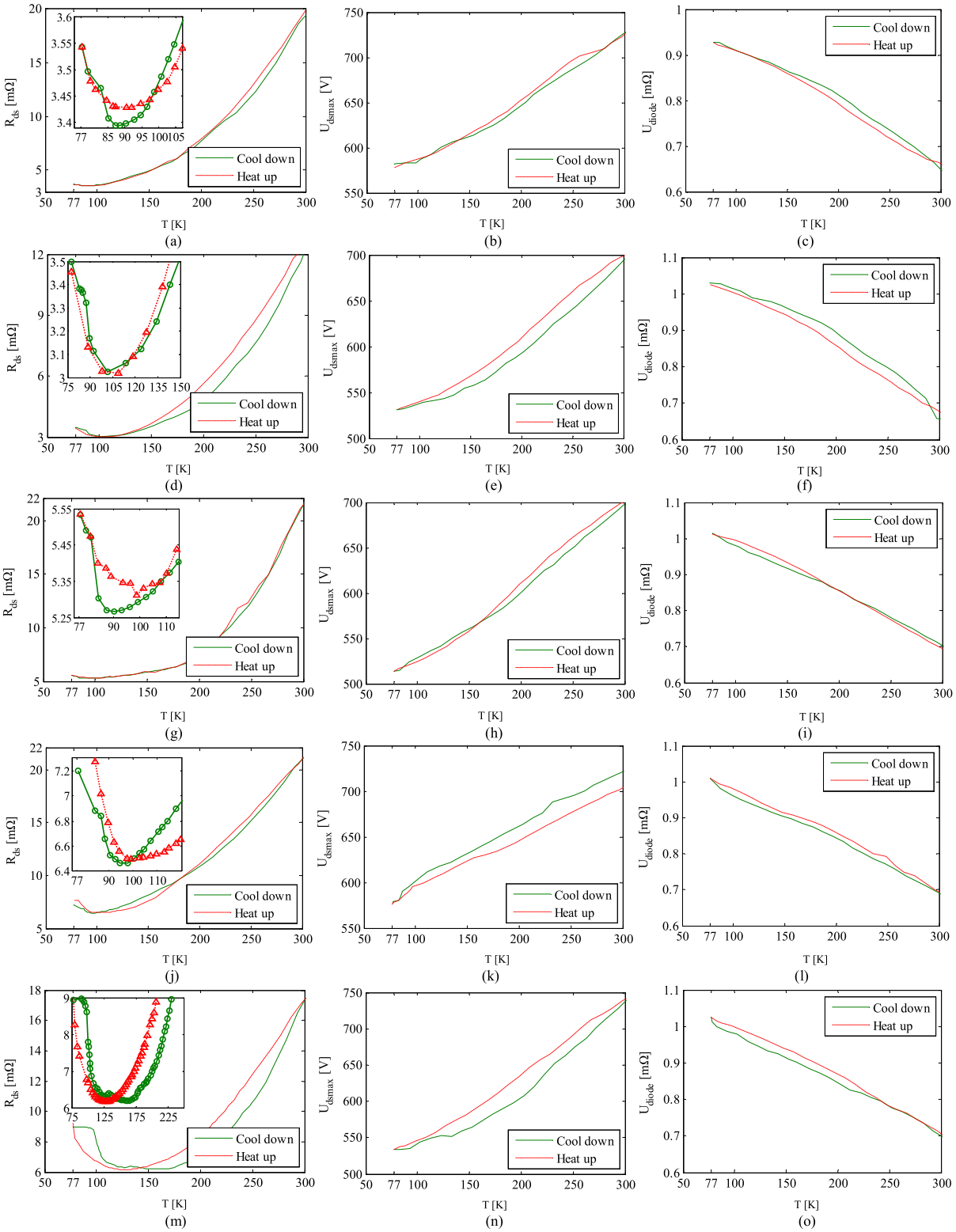


**FIGURE 3.** Low-current testing results in five types of power MOSFETs from 300 K to 77 K: (a) $R_{ds}$ in Type A; (b) $U_{dsmax}$ in Type A; (c) $U_{diode}$ test in Type A; (d) $R_{ds}$ in Type B; (e) $U_{dsmax}$ in Type B; (f) $U_{diode}$ in Type B; (g) $R_{ds}$ in Type C; (h) $U_{dsmax}$ in Type C; (i) $U_{diode}$ in Type C; (j) $R_{ds}$ in Type D; (k) $U_{dsmax}$ in Type D; (l) $U_{diode}$ in Type D; (m) $R_{ds}$ in Type E; (n) $U_{dsmax}$ in Type E; (o) $U_{diode}$ in Type E.

the optimal value. This is due to the combined effect of the temperature-dependent electron mobility and the ionised dopant concentration [18], [30]. In general, this optimum temperature range appears when both the highest electron mobility and the minimum effects of carrier freeze-out are achieved. Therefore, a suitable operating temperature range

should be properly selected for practical cryogenic power conversions.

### *B. FITTED MATHEMATICAL FUNCTIONS OF POWER MOSFETS*

To discuss the cryogenic behaviors of power MOSFETs from the view of engineering applications, four normalized parameters are introduced as follows: 1) the ratio of the $R_{ds}$ at an arbitrary temperature to the $R_{ds}$ at 300 K is defined as $R_{pu1}$; 2) the ratio of the $R_{ds}$ at an arbitrary temperature to the $R_{ds}$ at 77 K is defined as $R_{pu2}$; 3) the ratio of the $U_{dsmax}$ at an arbitrary temperature to the $U_{dsmax}$ at 300 K is defined as $U_{pu1}$; 4) the ratio of the $U_{diode}$ at an arbitrary temperature to the $U_{diode}$ at 300 K is defined as $U_{pu2}$.

Fig. 4 shows the normalized $R_{pu1}$ values from 300 K to 77 K. All the $R_{pu1}$ values in the five MOSFETs are found to have double-exponential functional relations with temperatures

$$R_{pu1} = p_1 \times \exp\left(p_2 \times \frac{T}{T_0}\right) + p_3 \times \exp\left(p_4 \times \frac{T}{T_0}\right) \quad (1)$$

where $T_0$ is a normalized temperature of 1 K, $p_1$ - $p_4$ are four fitted parameters that depend on the types of power MOSFETs. Table 1 summarizes the fitted parameters in the five MOSFETs. From the fitted light blue lines in Fig. 4, these fitted functions match well with the measured $R_{pu1}$ values.

**TABLE 1. Fitted parameters for the five MOSFETs from 300 K to 77 K.**

| MOSFETs | $p_1$ | $p_2$ | $p_3$ | $p_4$ |
|---|---|---|---|---|
| Type A | 0.5198 | -0.0278 | 0.0566 | 0.0096 |
| Type B | 0.5877 | -0.0162 | 0.0501 | 0.0099 |
| Type C | 0.3355 | -0.0066 | 0.0206 | 0.0128 |
| Type D | 1.8931 | -0.0372 | 0.1391 | 0.0066 |
| Type E | 2.7151 | -0.0281 | 0.1047 | 0.0076 |

For further clarifying the cryogenic on-state resistance behaviors near the optimal temperature range, five double-exponential functions are also fitted from 200 K to 77 K. The fitted parameters and lines are given in Table 2 and Fig. 4. By comparing the fitted lines for the normalized $R_{pu1}$ and $R_{pu2}$ values, the parameters in Table 2 have higher fitting accuracies if the five MOSFETs are just operated near the optimal temperature range in practice.

**TABLE 2. Fitted parameters for the five MOSFETs from 200 K to 77 K.**

| MOSFETs | $p_1$ | $p_2$ | $p_3$ | $p_4$ |
|---|---|---|---|---|
| Type A | 30.252 | -0.0634 | 0.4271 | 0.0077 |
| Type B | 4.3591 | -0.0268 | 0.2201 | 0.0097 |
| Type C | 85.372 | -0.0875 | 0.7409 | 0.0024 |
| Type D | 21.641 | -0.0549 | 0.4135 | 0.0068 |
| Type E | 4.9131 | -0.0274 | 0.2087 | 0.0074 |

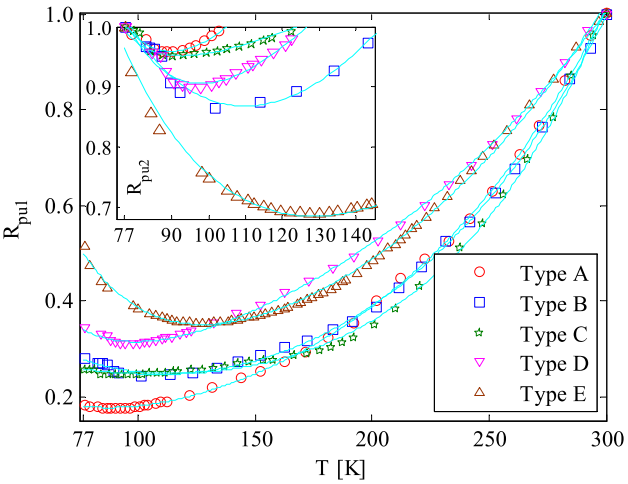


**FIGURE 4. Normalized $R_{pu1}$ and $R_{pu2}$ values and their fitted temperature-dependent double-exponential functions from 300 K to 77 K.**

Considering the nearly linear relations [5], [18], [25] among the $U_{dsmax}$, $U_{diode}$ and $T$, two linear functions are fitted as follows

$$U_{pu1} = p_5 \times \frac{T}{T_0} + p_6 \quad (2)$$

$$U_{pu2} = p_7 \times \frac{T}{T_0} + p_8 \quad (3)$$

where $p_5$ - $p_8$ are four fitted parameters that depend on the types of power MOSFETs. Table 3 summarizes the fitted parameters in the five MOSFETs.

**TABLE 3. Fitted parameters for the five MOSFETs from 300 K to 77 K.**

| MOSFETs | $p_5$ | $p_6$ | $p_7$ | $p_8$ |
|---|---|---|---|---|
| Type A | 0.6565 | 530.93 | -0.0012 | 1.0215 |
| Type B | 0.7391 | 473.79 | -0.0016 | 1.1469 |
| Type C | 0.8334 | 449.55 | -0.0014 | 1.1244 |
| Type D | 0.6461 | 527.44 | -0.0014 | 1.1208 |
| Type E | 0.9334 | 461.25 | -0.0014 | 1.1375 |

## IV. HIGH-CURRENT TESTS AND EFFICIENCY ANALYSES

### *A. CRYOGENIC ON-STATE RESISTANCE BEHAVIORS OF POWER MOSFETS IN HIGH-CURRENT TESTS*

As mentioned in Section III, cryogenic on-state resistance behaviors show some double-exponential functions with the operating temperature. Because of the relatively low testing current, power dissipation of one power MOSFET could be practically ignored during the tests. This means that the measured temperature data in Fig. 4 is approximately equal to the real junction temperature inside the MOSFET. Hence, the low-current testing results in Fig. 4 and their fitted mathematical functions in (1)-(3) could be considered as the ideal references for evaluating the temperature-dependent properties of cryogenic power MOSFETs.

However, it should be noted that the junction temperature might rise to be much higher than external ambient temperature when the operating current is increased to tens of amperes. This so-called self-heating effect [31]–[34] is easy to be found in the experiments when the MOSFET is not fully immersed in $LN_2$. Considering a suitable operating temperature range of 85-95 K found in Fig. 3(d), a 75-A DC current was applied to the Type-A MOSFET at 84.93 K in an experiment. After a 40-s testing time duration, the real-time temperature was measured to reach about 124.35 K. In contrast, when the MOSFET was fully immersed in $LN_2$, almost zero temperature rise was found in the same experiment. These phenomena reveal the fact that cryogenic power MOSFETs might not be maintained at a suitable operating temperature for high-current applications. The generated heat can not be completely taken away, and thus results in an ever-increasing temperature rise inside the MOSFET. This is mainly due to the limited cooling power from the cold-conduction strip and limited thermal conductivity from the existing MOSFET structure. Therefore, although all the optimal temperature values found in Fig. 4 are higher than the $LN_2$ temperature, cryogenic power MOSFETs should be practically immersed in $LN_2$ for high-current operations.

Fig. 5 shows the high-current testing results in the fiver MOSFETs at 77 K. Note that the testing time $t$ in the left vertical axis is denoted for those high current tests ranged from 20 A to 90 A, while the operating temperature $T$ in the right vertical axis is just used for the low-current tests at 4 A. For comparing the cryogenic on-state resistance behaviors in the low-current and high-current tests, all the measured on-state resistances are normalized by using the concept of $R_{pu1}$. It can be seen that the $R_{pu1}$ increases firstly and then decreases as the operating current $I_{ds}$ increases from 20 A to 90 A. The reason is that practical cooling power for the semiconductor materials inside the MOSFET is still limited even when the whole MOSFET is immersed in $LN_2$. These phenomena reveal the fact that minimum power dissipation at 77 K can be achieved when cryogenic power MOSFETs are operated at a moderate current, e.g., 50-60 A in Type-A and Type-B MOSFETs.

Specifically, when the operating current is relatively low, i.e., the power dissipation is lower than the maximum cooling power, practical junction temperature might be maintained at 77 K or a slightly higher value. However, when the operating current is relatively high, an obvious junction temperature rise will be caused by the surplus heat accumulation from the self-heating effects [31]–[34]. Thanks to the directly proportional relation between the thermal conductivity and operating temperature of the semiconductor materials [31], [35], the corresponding thermal conductivity shows an increasing trend along with the temperature rise, and thus results in an enhancement for practical cooling power. Finally, the operating junction temperature will reach a steady value when a dynamic power balance is achieved. This steady temperature value can be obtained by using the relations among the normalized on-state resistance, operating current and temperature. From Fig. 5, the $R_{pu1}$ are basically stabilized at $t = 40$ s. Hence the corresponding coordinate values in the right vertical axis are the practical junction temperatures. For instance, the measured power dissipation of Type-A MOSFET is about 30 W at 90 A,

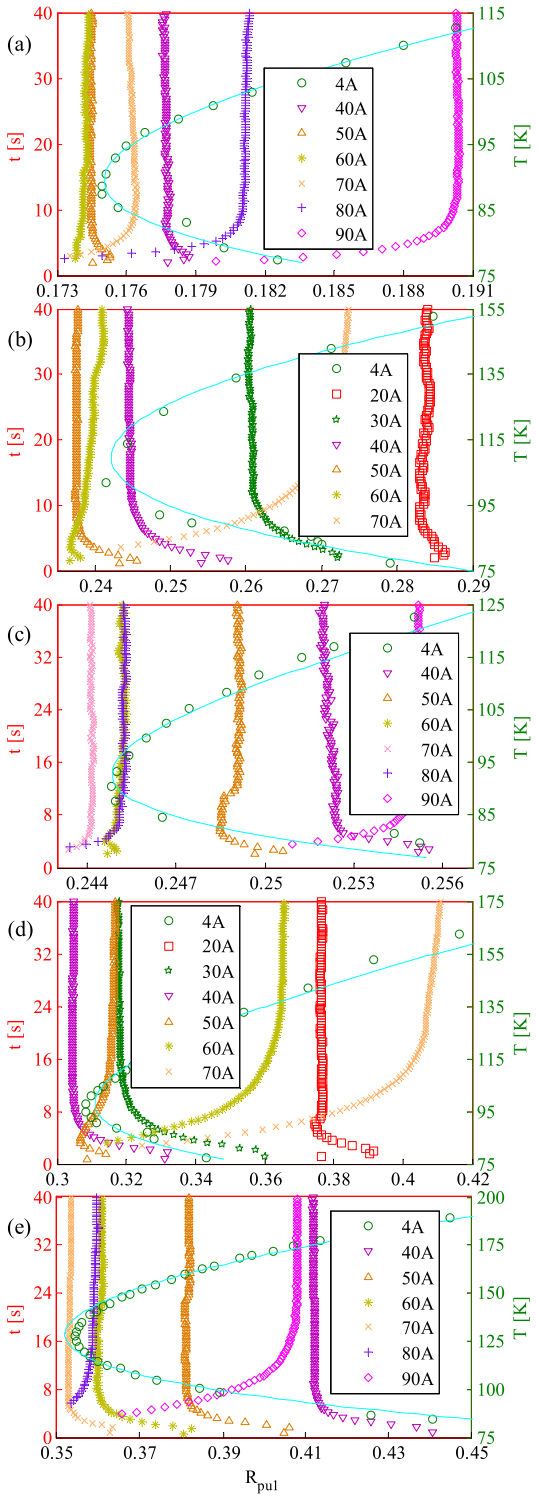


**FIGURE 5. High-current testing results in five types of power MOSFETs at 77 K: (a) Type A; (b) Type B; (c) Type C; (d) Type D; (e) Type E.**

and its corresponding junction temperature can be estimated to be about 111 K by reference to Fig. 5(a). Accordingly, the measured on-state resistance of about 3.69 mΩ in this high-current test also matches well with the low-current testing result and double-exponential functional relation. However, if the thermal resistance of 0.1 K/W given in the official data sheet is simply used to estimate the junction temperature, the calculated temperature rise is only about 3 K.

### *B. ENERGY EFFICIENCY ANALYSES OF CRYOGENIC POWER MOSFETS*

To evaluate the cryogenic on-state resistance behaviors in high-current tests, the relations between the stabilized on-state resistances and operating currents are extracted from Fig. 5 and summarized in Fig. 6. Since the stabilized junction temperatures are directly related to the operating currents, the double-exponential function in (1) can also be used to depict the current-resistance relations at 77 K

$$R_{\mathrm{pu1}} = p_9 \times \exp\left(p_{10} \times \frac{I_{\mathrm{ds}}}{I_0}\right) + p_{11} \times \exp\left(p_{12} \times \frac{I_{\mathrm{ds}}}{I_0}\right) \quad (4)$$

where $I_0$ is a normalized temperature of 1 A, $p_9 - p_{12}$ are four fitted parameters that depend on the types of power MOSFETs. Table 4 summarizes the fitted parameters in the five MOSFETs. These results and their fitted current-dependent functions can be used to estimate the power dissipations of cryogenic power MOSFETs under high-current operations.

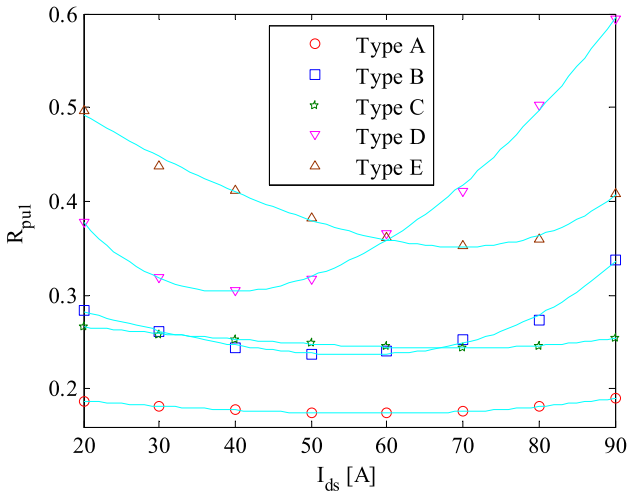


**FIGURE 6.** Normalized $R_{\mathrm{pu1}}$ values and their fitted current-dependent double-exponential functions at 77 K.

From the definition of $R_{\mathrm{pu1}}$ introduced in Section III, the $R_{\mathrm{pu1}}$ values in Fig. 6 are obtained by dividing the cryogenic on-state resistances at 77 K by their room-temperature counterparts at 300 K. However, if one MOSFET at room temperature is operated at a high current, practical junction temperature will certainly be stabilized at a higher value. Similar to the cryogenic on-state behaviors at 77 K, this temperature-rise phenomenon is also due to the imbalance between the cooling power and power dissipation inside the MOSFET.

**TABLE 4.** Fitted parameters for the five MOSFETs at 77 K.

| MOSFETs | $p_9$ | $p_{10}$ | $p_{11}$ | $p_{12}$ |
|---|---|---|---|---|
| Type A | 0.1966 | -0.0052 | 0.0061 | 0.0267 |
| Type B | 0.3308 | -0.0093 | 0.0031 | 0.0463 |
| Type C | 0.2811 | -0.0031 | 0.0006 | 0.0459 |
| Type D | 0.6366 | -0.0526 | 0.1053 | 0.0191 |
| Type E | 0.5981 | -0.0102 | 0.0014 | 0.0529 |

To evaluate the energy efficiency of cryogenic power MOSFETs as accurately as possible, a new normalized on-state resistance $R_{\mathrm{pu3}}$ is introduced by dividing the cryogenic on-state resistance at 77 K by its room-temperature counterpart above 300 K. From the official data sheets of the five MOSFETs, their on-state resistances show almost linear ascending trends with increased junction temperatures above 300 K. Practical junction temperatures under such a room-temperature condition are mainly determined by the operating currents and heat dissipation properties of heat sinks. In general, the maximum junction temperature must be lower than 150 °C. In the cases of high-current operations, practical junction temperatures could be assumed to be in the range from 25 °C to 145 °C. The corresponding on-state resistances given in the official data sheets are hence used to estimate the $R_{\mathrm{pu3}}$ values when a series of DC testing currents are applied to the MOSFETs at 77 K.

Fig. 7 shows the relations among the normalized on-state resistances, operating currents and junction temperatures in the five MOSFETs. It can be seen that the $R_{\mathrm{pu3}}$ at an arbitrary operating current shows almost linear descending trends with increased temperatures above 300 K. Considering the linear relation between the power dissipation and on-state resistance, the reduced $R_{\mathrm{pu3}}$ values in Fig. 7 result in much lower power dissipations. This means that the energy efficiencies of cryogenic power MOSFETs themselves are much improved compared to their room-temperature counterparts.

However, under such a cryogenic environment at 77 K, a concept of Carnot refrigerating efficiency should be introduced to evaluate the overall energy efficiency by considering both the reduced power dissipations from the MOSFETs and the increased refrigerating power from their equipped refrigerators. The ideal Carnot refrigerating efficiency is about 34.77% at 77 K. To generate the $LN_2$ in large quantities or keep the existing $LN_2$ at 77 K, a possible Carnot refrigerating efficiency $\eta_{\mathrm{cold}}$ could reach about 17.38% at maximum [23]. This means that about 5.75-W electrical power at room temperature is practically consumed to produce 1-W cooling power at 77 K. For achieving an improved energy efficiency of the whole cryogenic power conversion system, the reference flat surfaces ($\eta_{\mathrm{cold}} = 17.38\%$) in Fig. 7 depict vividly the suitable operating areas. Specifically,

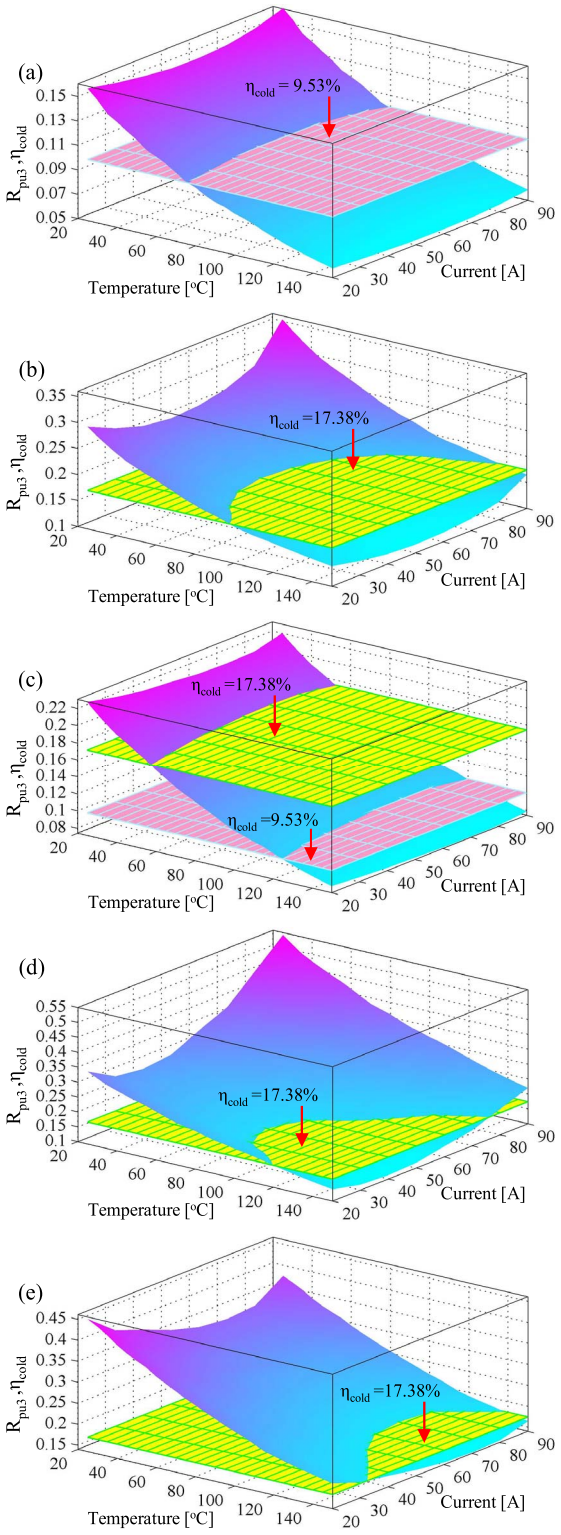


**FIGURE 7.** **Relations among the normalized on-state resistances, operating currents and junction temperatures in the five types of power MOSFETs: (a) Type A; (b) Type B; (c) Type C; (d) Type D; (e) Type E.**

these suitable operating areas are obtained when the curved surfaces are below the reference flat surfaces. As shown in Fig. 7, all the five MOSFETs have some suitable operating areas if the Carnot refrigerating efficiency $\eta_{cold}$ could reach about 17.38%.

However, based on the product investigations of various refrigerator manufacturers, the maximum Carnot refrigerating efficiency is only about 9.53% among commercial cryogenic refrigerators at present. This maximum efficiency is achieved in a Stirling Process Cryogenerator (SPC-4) manufactured by Stirling Cryogenics. Its input power is rated at 43 kW for producing a cooling power of 4.1 kW at 77 K. Hence, for achieving an improved energy efficiency, the $R_{pu3}$ values should be less than this existing efficiency of 9.53%. As shown in Fig. 7, only the two curved surfaces in Type-A and Type-C MOSFETs are found to have some suitable operating areas. When the practical operating junction temperature under a room-temperature condition is above about 60 °C in Type-A MOSFET or above about 120 °C in Type-C MOSFET, cryogenic operations of these two MOSFETs have higher energy efficiencies over their room-temperature counterparts.

## V. DESIGN GUIDELINES AND CASE STUDIES OF CRYOGENIC POWER CONVERSIONS AT 77 K

### *A. DESIGN GUIDELINES OF CRYOGENIC POWER CONVERSIONS*

Benefited from good fitting effects in Figs. 3-6, the four fitted mathematical functions in (1)-(4) can be well expected to form a feasible design guideline for cryogenic power conversions at 77 K. As shown in Fig. 8, its main design procedures are as follows.

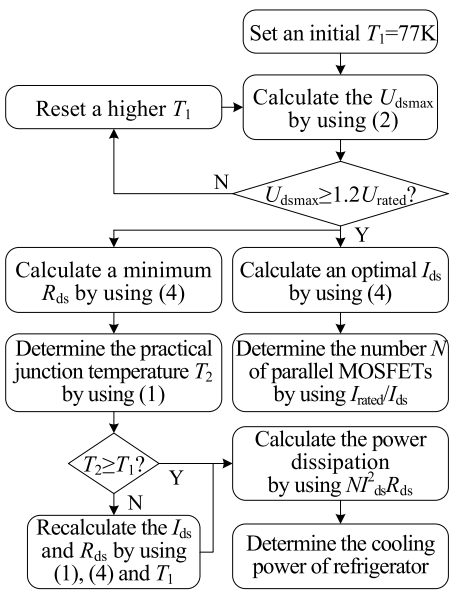


**FIGURE 8.** **A feasible design guideline of cryogenic power conversions at 77 K.**

1) Measure the cryogenic operating data of the $R_{ds}$, $U_{dsmax}$ and $U_{diode}$ in both the low-current and high-current tests, and then update the fitted parameters in (1)-(4).

2) Set an initial junction temperature $T_1 = 77$ K when the MOSFETs are fully immersed in $LN_2$, and then calculate the $U_{dsmax}$ at 77 K by using (2).

3) Set a safety margin of 1.2 times of the rated operating voltage $U_{rated}$, and then compare the $U_{dsmax}$ and $1.2U_{rated}$ to determine whether the $U_{dsmax}$ at 77 K meets the voltage demand or should be further improved by resetting a higher $T_1$.

4) Once the $U_{dsmax}$ is equal to or higher than $1.2U_{rated}$ at 77 K or a higher $T_1$, the minimum $R_{ds}$ and its corresponding optimal $I_{ds}$ can be calculated by using (4).

5) With the minimum $R_{ds}$ and optimal $I_{ds}$ values, the practical junction temperature $T_2$ and the round number $N$ of parallel-connected MOSFETs can be determined by using (2) and a ratio of the rated operating current $I_{rated}$ to the optimal $I_{ds}$, respectively.

6) When the calculated $T_2$ value is equal to or higher than the pre-set $T_1$ value, the power dissipation can be calculated by using $NI_{ds}^2R_{ds}$; however, when the calculated $T_2$ value is lower than the pre-set $T_1$ value, practically allowable $R_{ds}$ and $I_{ds}$ values should be re-calculated by using (1), (4) and $T_1$.

7) Considering the total power dissipation from all the MOSFET assemblies inside the whole cryogenic power system, a minimum cooling power can be determined for the use in the practical selections of commercial cryogenic refrigerators.

With the above seven design procedures, a cryogenic power conversion system can be basically designed for prototype development. In cases when the built-in reverse diodes or some other standalone power diodes are involved into the operations of cryogenic power conversion, the $U_{diode}$ at 77 K should also be calculated by using (3). This $U_{diode}$ value is then further used to estimate the power dissipations from the diodes and to update the cooling power requirement for the cryogenic refrigerators. However, it is very uneconomical to operate the diodes at 77 K due to their increased power dissipations at lower temperatures. Therefore, replacing the power diodes by cryogenic power MOSFETs could be an energy-saving choice.

### B. CASE STUDIES ON CRYOGENIC POWER CONVERSIONS AT 77 K

For a typical application case in the 40-kW cryogenic boost chopper reported in [24], two Type-A cryogenic power MOSFETs are used to replace one room-temperature power MOSFET and one power diode in the conventional boost chopper. In this cryogenic power conversion case, the output voltage from a 200-V/200-A DC source is boosted to supply a 400-V/200-A resistive load. Hence the rated voltage $U_{rated}$ and rated current $I_{rated}$ in each MOSFET are about 400 V and 200 A, respectively. Considering a safety margin of 1.2 times of the rated voltage, the $U_{dsmax}$ in each MOSFET should be with $\geq$480 V at 77 K. By reference to (2), the calculated $U_{dsmax}$ value is about 581 V at 77 K. This means that the Type-A MOSFET meets the operating voltage requirement from the 40-kW cryogenic boost chopper even when the junction temperature is exactly equal to 77 K.

By using (4), the minimum $R_{ds}$ and its corresponding optimal $I_{ds}$ are estimated to be about 3.39 m$\Omega$ and 50 A, respectively. Hence, four Type-A MOSFETs should be connected in parallel to form a switching assembly for carrying a total current of 200 A, and the practical junction temperature at 50 A is estimated to be about 90 K by using (1). This junction temperature value corresponds to an increased $U_{dsmax}$ of about 590 V in the 40-kW cryogenic boost chopper.

Finally, considering a duty cycle of 50% in each MOSFET assembly, the total power dissipation from the two MOSFET assemblies is calculated to be about 33.9 W. Even when the operating loss from the HTS inductor is taken into account, the total loss is only about 42.8 W. Hence, an AL60-type Gifford-McMahon (GM) refrigerator manufactured by Cryomech could be a suitable cooling choice. Its input power is rated at 1.7 kW for producing a cooling power of 49.1 W at 77 K. By considering the Carnot refrigerating efficiency of 2.89% in this refrigerator, practical power consumed in room temperature should be about 1482 W in total. This results in a high energy efficiency of 96.43% for the whole 40-kW chopper system. However, such a cryogenic power conversion system having relatively low operating current and power is uneconomical in practice. Considering a capital cost per unit cooling power of about 25 \$/W at 77 K [36], the refrigerator itself needs an additional cost of about \$1228.

Fortunately, cryogenic power conversions could be well expected to have promising advantages in those high-power high-efficiency high-quality power conversions [37] such as in renewable energy systems, superconducting DC power network and Internet data centers. For instance, if the 40-kW chopper is extended to have a high power of 4 MW for the use in Internet data center, four hundred of Type-A MOSFETs should be connected in parallel to carry a nearly steady current of 20 kA. The total power dissipation in the 4-MW chopper is about 3390 W at 77 K. Hence the SPC-4 refrigerator with a high efficiency of 9.53% could be applied to maintain the whole chopper at 77 K. The total energy efficiency is estimated to be about 99.12%. Although this value is only slightly higher than the room-temperature efficiency of about 98.92%, such a 4-MW cryogenic power conversion has several promising application advantages as follows: 1) elimination of large-volume and heavy-weight drawbacks in conventional air or water cooled devices; 2) elimination of potential overheating risks in power MOSFETs; 3) permission of high current and power ratings; 4) adaptability of high power quality.

## VI. CONCLUSION

An up-to-date experimental investigation into five types of 650 V class power MOSFETs has been presented to explore a possible design guideline for cryogenic power conversions at 77 K. Based on the integrated analyses of experimental results, conclusions can be made as follows.

1) The measured on-state resistance obtained in low-current tests shows almost double-exponential functional relations with the operating temperature, while the other two cryogenic parameters are directly or inversely proportional to the operating temperature.

2) Although all the optimal temperature values found in the low-current tests are somewhat higher than 77 K, cryogenic power MOSFETs should be practically operated at 77 K for high-current operations by considering the limited thermal conductivity and its resulting self-heating effect from the existing MOSFET structure. Cryogenic on-state resistance behaviors in the high-current tests from 20 A to 90 A are also found to have double-exponential functional relations with the operating current. This means that the minimum power dissipation at 77 K can be achieved at a moderate current, e.g., 50-60 A in Type-A and Type-B MOSFETs.

3) The current-temperature-resistance correspondences found in the temperature-dependent and current-dependent functions lay some empirical bases to design and evaluate the suitable operating current and voltage ratings of cryogenic power MOSFETs at 77 K, and thus to form a feasible design guideline for the use in various cryogenic power conversions.

4) Considering the maximum Carnot refrigerating efficiency of about 9.53% among state-of-the-art commercial refrigerators, cryogenic operations of Type-A and Type-C MOSFETs have higher energy efficiencies compared to their room-temperature counterparts at present. Along with the developments of the unceasingly mature refrigerators and cryogenically preferable power MOSFETs in near future, cryogenic power conversions can be well expected to become promising alternatives, especially for the use in high-power high-efficiency high-quality power conversion applications.

## REFERENCES

[1] K. Rajashekara and B. Akin, "Cryogenic power conversion systems: The next step in the evolution of power electronics technology," *IEEE Electrification Mag.*, vol. 1, no. 2, pp. 64–73, Dec. 2013.

[2] K. A. Wilson, P. L. Tuxbury, and R. L. Anderson, "A simple analytical model for the electrical characteristics of depletion-mode MOSFET's with application to low-temperature operation," *IEEE Trans. Electron Devices*, vol. 33, no. 11, pp. 1731–1737, Nov. 1986.

[3] O. Mueller, "On-resistance, thermal resistance and reverse recovery time of power MOSFETs at 77 K," *Cryogenics*, vol. 29, no. 10, pp. 1006–1014, Oct. 1989.

[4] R. Karunanithi, A. K. Raychaudhuri, Z. Szücs, and G. V. Shivashankar, "Behaviour of power MOSFETs at cryogenic temperatures," *Cryogenics*, vol. 31, no. 12, pp. 1065–1069, Dec. 1991.

[5] R. Singh and B. J. Baliga, "Analysis and optimization of power MOSFETs for cryogenic operation," *Solid State Electron.*, vol. 36, no. 8, pp. 1203–1211, Aug. 1993.

[6] P. Ghazavi and F. D. Ho, "A numerical model for MOSFET's from liquid-nitrogen temperature to room temperature," *IEEE Trans. Electron Devices*, vol. 42, no. 1, pp. 123–134, Jan. 1995.

[7] R. J. Mauriello, K. B. Sundaram, and L. C. Chowb, "Simulation of Si power MOSFET under cryogenic conditions," *Solid State Electron.*, vol. 43, no. 4, pp. 771–777, Apr. 1999.

[8] R. J. Mauriello, K. B. Sundaram, and L. C. Chow, "A study of on-resistance and switching characteristics of the power MOSFET under cryogenic conditions," *Int. J. Electron.*, vol. 87, no. 1, pp. 99–106, Nov. 2000.

[9] P. Haldar *et al.*, "Improving performance of cryogenic power electronics," *IEEE Trans. Appl. Supercond.*, vol. 15, no. 2, pp. 2370–2375, Jun. 2005.

[10] A. Akturk *et al.*, "Compact and distributed modeling of cryogenic bulk MOSFET operation," *IEEE Trans. Electron Devices*, vol. 57, no. 6, pp. 1334–1342, Jun. 2010.

[11] Z. Zhu *et al.*, "Design applications of compact MOSFET model for extended temperature range (60–400k)," *Electron. Lett.*, vol. 47, no. 2, pp. 141–142, Jan. 2011.

[12] T. Curcic and S. A. Wolf, "Superconducting hybrid power electronics for military systems," *IEEE Trans. Appl. Supercond.*, vol. 15, no. 2, pp. 2364–2369, Jun. 2005.

[13] P. Pereira *et al.*, "Power electronics performance in cryogenic environment: Evaluation for use in HTS power devices," *J. Phys. Conf.*, vol. 97, Mar. 2008, Art. no. 012219.

[14] Y. Kondo, S. Fukano, A. Ninomiya, and T. Ishigohka, "Cryogenic low-voltage/high-current DC power source using multi-parallel-connected MOSFETs," *IEEE Trans. Appl. Supercond.*, vol. 19, no. 3, pp. 2337–2340, Jun. 2009.

[15] W. Bailey, H. Wen, Y. Yang, A. Forsyth, and C. Jia, "A cryogenic dc-dc power converter for a 100 kW synchronous HTS generator at liquid nitrogen temperatures," *Phys. Proc.*, vol. 36, pp. 1002–1007, Jun. 2012.

[16] A. J. Forsyth *et al.*, "Cryogenic converter for superconducting coil control," *IET Power Electron.*, vol. 5, no. 6, pp. 739–746, Jul. 2012.

[17] J. X. Jin, X. Y. Chen, L. Wen, S. C. Wang, and Y. Xin, "Cryogenic power conversion for SMES application in a liquid hydrogen powered fuel cell electric vehicle," *IEEE Trans. Appl. Supercond.*, vol. 25, no. 1, p. 11, Feb. 2015.

[18] K. K. Leong, B. T. Donnellan, A. T. Bryant, and P. A. Mawby, "An investigation into the utilisation of power MOSFETs at cryogenic temperatures to achieve ultra-low power losses," in *Proc. IEEE Energy Convers. Congr. Expo.*, Atlanta, GA, USA, Sep. 2010, pp. 2214–2221.

[19] K. K. Leong, A. T. Bryant, and P. A. Mawby, "Power MOSFET operation at cryogenic temperatures: Comparison between HEXFET®, MDMesh™ and CoolMOS™," in *Proc. Int. Symp. Power Semicond. Devices ICs*, Hiroshima, Japan, Jun. 2010, pp. 209–212.

[20] F. F. Perez-Guerrero, B. Ray, and R. L. Patterson, "Low temperature operation of a three-level buck DC-DC converter," in *Proc. 32nd Intersoc. Energy Convers. Eng. Conf.*, Honolulu, HI, USA, Aug. 1997, pp. 1415–1420.

[21] H. Li, D. Liu, and C. A. Luongo, "Investigation of potential benefits of MOSFETs hard-switching and soft-switching converters at cryogenic temperature," *IEEE Trans. Appl. Supercond.*, vol. 15, no. 2, pp. 2376–2380, Jun. 2005.

[22] C. Jia and A. J. Forsyth, "Evaluation of semiconductor losses in cryogenic DC-DC converters," in *Proc. 5th Int. Power Electron. Motion Control Conf.*, Shanghai, China, Aug. 2006, pp. 1–5.

[23] O. M. Mueller and K. G. Herd, "Ultra-high efficiency power conversion using cryogenic MOSFETs and HT-superconductors," in *Proc. IEEE Power Electron. Specialists Conf.*, Seattle, WA, USA, Jun. 1993, pp. 772–778.

[24] X. Y. Chen *et al.*, "An efficient boost chopper integrated with cryogenic MOSFETs and HTS inductor," *IEEE Trans. Appl. Supercond.*, vol. 26, no. 7, p. 6, Oct. 2016.

[25] R. Singh and B. J. Baliga, "Power MOSFET analysis/optimization for cryogenic operation including the effect of degradation in breakdown voltage," in *Proc. Int. Symp Power Semicond. Devices ICs*, Tokyo, Japan, 1992, pp. 339–344.

[26] R. J. Mauriello, K. B. Sundaram, and L. C. Chow, "Simulation of Si power MOSFET under cryogenic conditions," *Solid State Electron.*, vol. 43, no. 4, pp. 771–777, Apr. 1999.

[27] H. Ye *et al.*, "Silicon power MOSFET at low temperatures: A two-dimensional computer simulation study," *Cryogenics*, vol. 47, no. 4, pp. 243–251, Apr. 2007.

[28] A. Kabaoğlu and M. B. Yelten, "A cryogenic modeling methodology of MOSFET I-V characteristics in BSIM3," in *Proc. 14th Int. Conf. Synth. Model. Anal. Simulat. Methods Appl. Circuit Design*, Giardini Naxos, Italy, Jun. 2017, pp. 1–4.

[29] M. Giesselmann, Z. Mahund, and S. Carson, "Investigation of power MOSFET switching at cryogenic temperatures," in *Proc. 22nd Int. Power Modulator Symp.*, Boca Raton, FL, USA, Jun. 1996, pp. 47–50.

[30] C. Jacoboni, C. Canali, G. Ottaviani, and A. A. Quaranta, "A review of some charge transport properties of silicon," *Solid State Electron.*, vol. 20, no. 2, pp. 77–89, Feb. 1977.
[31] D. P. Foty and S. L. Titcomb, "Thermal effects in n-channel enhancement MOSFET's operated at cryogenic temperatures," *IEEE Trans. Electron Devices*, vol. 34, no. 1, pp. 107–113, Jan. 1987.
[32] E. A. Gutiérrez D., L. Deferm, and G. Declerck, "Selfheating effects in silicon resistors operated at cryogenic ambient temperatures," *Solid State Electron.*, vol. 36, no. 1, pp. 41–52, Jan. 1993.
[33] F. J. De la Hidalga, M. J. Deen, and E. A. Gutierrez, "Theoretical and experimental characterization of self-heating in silicon integrated devices operating at low temperatures," *IEEE Trans. Electron Devices*, vol. 47, no. 5, pp. 1098–1106, May 2000.
[34] T. Takahashi, T. Matsuki, T. Shinada, Y. Inoue, and K. Uchida, "Direct evaluation of self-heating effects in bulk and ultra-thin BOX SOI MOSFETs using four-terminal gate resistance technique," *IEEE J. Electron Devices Soc.*, vol. 4, no. 5, pp. 365–373, Sep. 2016.
[35] J. C. Thomson and B. A. Younglove, "Thermal conductivity of silicon at low temperatures," *J. Phys. Chem. Solids*, vol. 20, nos. 1–2, pp. 146–149, Jun. 1961.
[36] B. Gromoll, "Technical and economical demands on 25 K—7 K refrigerators for future HTS—Series products in power engineering," *AIP Conf. Proc.*, vol. 710, no. 1, pp. 1797–1804, Jul. 2004.
[37] X. Y. Chen and J. X. Jin, "Energy efficiency analysis and energy management of a superconducting LVDC network," *IEEE Trans. Appl. Supercond.*, vol. 26, no. 7, p. 5, Oct. 2016.

**YU CHEN** is currently pursuing the B.S. degree in electrical engineering with Sichuan Normal University, Chengdu, China.

**XIAO-YUAN CHEN** received the B.S. degree from the Chengdu University of Technology, Chengdu, China, in 2007 and the Ph.D. degree from the University of Electronic Science and Technology of China, Chengdu, in 2015. He is currently a Lecturer with the School of Engineering, Sichuan Normal University, Chengdu. His research interests include low-voltage direct-current superconducting power transmission and distribution, hybrid electrical-chemical energy transfer and utilization, and cryogenic power electronics.

**TAO LI** is currently pursuing the B.S. degree in electrical engineering with Sichuan Normal University, Chengdu, China.

**YING-JUN FENG** is currently pursuing the B.S. degree in electrical engineering with Sichuan Normal University, Chengdu, China.

**YANG LIU** is currently pursuing the B.S. degree in electrical engineering with Sichuan Normal University, Chengdu, China.

**QIN HUANG** is currently pursuing the B.S. degree in electrical engineering with Sichuan Normal University, Chengdu, China.

**MENG-YAO LI** received the B.S. degree from Sichuan Technology and Business University, Chengdu, China, in 2017. She is currently pursuing the M.S. degree in safety engineering with Sichuan Normal University, Chengdu.

**LEI ZENG** received the B.S. degree from Sichuan Normal University, Chengdu, China, in 2017, where she is currently pursuing the M.S. degree in safety engineering.